

Direct calculation of the moments of the distribution of photon time of flight in tissue with a finite-element method

Simon R. Arridge and Martin Schweiger

Modeling of the full temporal behavior of photons propagating in diffusive materials is computationally costly. Rather than deriving intensity as a function of time to fine sampling, we may consider methods that derive a transform of this function. To derive the Fourier transform involves calculation in the (complex) frequency domain and relates to intensity-modulated experiments. We consider instead the Mellin transform and show that this relates to the moments of the original temporal distribution. A derivation of the Mellin transform given the Fourier transform that permits closed-form derivations of the temporal moments for various simple geometries is presented. For general geometries a finite-element method is presented, and it is demonstrated that the computational cost to produce the n th moment is the same as producing the first n temporal samples of the original function.

1. Introduction

The measurement of time of flight of photons in tissue, using methods that use ultrashort light pulses and a fast optical detector,^{1,2} is a rapidly growing area. Biological tissue is a highly light-scattering medium, and the light that is detected in such studies has traveled considerably farther through the tissues than the direct distance between the input and output optodes. To quantify spectral information, it is necessary to know this optical path length, and the way in which it changes with tissue type, wavelength, attenuation, and measuring geometry.

It is of great importance to have a reliable model that can compute the form of the output intensity $\Gamma(t)$ for any given experimental situation. Such models are used, for example, in fitting to experimental data to determine global values of optical parameters³ and in image-reconstruction algorithms.⁴ Models are either stochastic, such as the Monte Carlo⁵⁻⁷ or random-walk⁸ models, which follow individual photon histories, or deterministic, based on a partial differential

equation for photon density. Whereas the former are arguably more closely related to the physics of the situation, the latter are clearly preferable in the development of analytic methods. Deterministic models can sometimes be solved analytically, for example, for simple geometries and homogeneous values of optical parameters,⁹ but for general geometries, or for inhomogeneous distributions of optical parameters, a numerical method is required, of which a powerful, robust, and efficient example is the finite-element method (FEM).¹⁰ Figure 1 shows an example of $\Gamma(t)$ produced from a two-dimensional FEM model of a 25-mm-radius circle, at 800 time steps of 5 ps, in 5290 s (see Table 1, below, and Section 4 for details).

In general, all methods for deriving $\Gamma(t)$ in non-trivial cases are computationally intensive. By contrast, calculation of $\hat{\Gamma}(\omega)$ is often much simpler. Sampling $\hat{\Gamma}(\omega)$ at a set of n frequencies spaced by $\Delta\omega$, including the dc signal ($\omega = 0$) and up to the Nyquist frequency ω_N , would be equivalent to sampling the time-domain signal at a space of $2\pi/\omega_N$. Computation of $\Gamma(t)$ could conceivably be carried out by solution in the Fourier domain followed by an inverse Fourier transform, but it is not clear that significant advantage would be gained in computation time. Because $\Gamma(t)$ for most biological subjects tends to have the very characteristic shape shown in Fig. 1, with positive skew and kurtosis, the question arises whether the function itself is really required or whether some description or statistic of the function

S. R. Arridge is with the Department of Computer Science, University College London, Gower Street, London, WC1E 6BT. M. Schweiger is with the Department of Medical Physics and Bioengineering, University College London, Capper Street, London WC1E 6JA.

Received 17 May 1994; revised manuscript received 8 September 1994.

0003-6935/95/152683-05\$06.00/0.

© 1995 Optical Society of America.

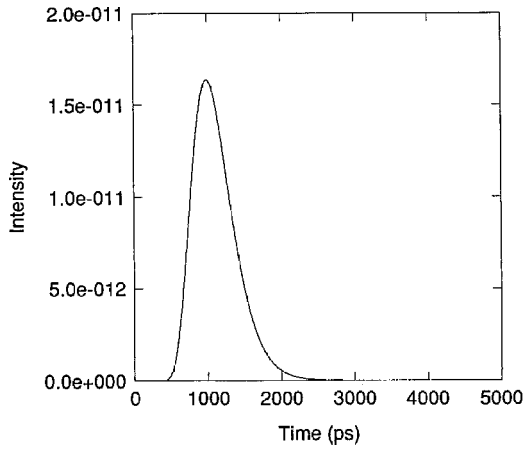


Fig. 1. $\Gamma(t)$ at an angle of 86° from δ function source on a two-dimensional circle, radius 25 mm, $\mu_a = 0.025 \text{ mm}^{-1}$, $\mu_s' = 2.0 \text{ mm}^{-1}$.

would provide the information needed. For example, many workers advocate measurement directly in the frequency domain of an intensity-modulated signal and consideration of the phase Ψ and the modulation depth M at particular frequencies. Then reproduction of a typical picosecond laser experiment, sampled at 10-ps intervals, would require sampling in the frequency domain up to several gigahertz, which is not practical with current technology.

Alternatively, instead of the Fourier transform, we can consider the Mellin transform:

$$\Gamma^*(s) = M[\Gamma(t); s] = \int_0^\infty t^{s-1} \Gamma(t) dt. \quad (1)$$

Calculation of $\Gamma^*(s)$ for integer $s > 1$ makes it straightforward to derive the moments of the temporal distribution:

$$\begin{aligned} \langle t^n \rangle &= \frac{\int_0^\infty t^n \Gamma(t) dt}{\int_0^\infty \Gamma(t) dt} = \frac{\Gamma^*(n+1)}{\Gamma^*(1)}, \\ \sigma_0 &= \Gamma^*(1), \quad \sigma_1 = \langle t \rangle, \\ \sigma_n &= \frac{\int_0^\infty (t - \langle t \rangle)^n \Gamma(t) dt}{\int_0^\infty \Gamma(t) dt} \\ &= \sum_{j=0}^n (-1)^{n-j} \binom{n}{j} \langle t^j \rangle \sigma_1^{(n-j)} \quad (n > 1). \end{aligned} \quad (2)$$

From Eqs. (2) one can derive statistical measures such as integrated intensity ($E = \sigma_0$), mean time ($\langle t \rangle = \sigma_1$), standard deviation ($\sqrt{\sigma_2}$), skew ($\sigma_3/\sigma_2^{3/2}$),

and kurtosis [$(\sigma_4/\sigma_2^2) - 3$]. In the temporal domain, the mean time σ_1 has been shown experimentally and theoretically to correspond to the differential path that relates the rate of change of measured intensity to change in absorption. The difference between $\omega\sigma_1$ and Ψ is to a first approximation dependent on the skew of $\Gamma(t)$.⁹ Moments have been used successfully in an image-reconstruction algorithm.¹¹

The optimal statistics of $\Gamma(t)$ to use for data analysis is still a matter of investigation. The purpose of this paper is to report a computationally efficient method for deriving the moments directly without having to evaluate $\Gamma(t)$. This method permits the use of the moments as an alternative to direct sampling of $\Gamma(t)$ or of $\hat{\Gamma}(\omega)$. We give the analytic form and the form suitable for finite elements. In the latter case the computational cost to produce the n th moment is the same as producing the first n temporal samples of $\Gamma(t)$. We compare analytic results with FEM results and with the numerical integration of $\Gamma(t)$.

2. Light Transport

We consider our model of light transport to be the diffusion equation:

$$\left\{ \nabla \cdot \kappa(\mathbf{r}) \nabla - \mu_a(\mathbf{r})c - \frac{\partial}{\partial t} \right\} \Phi(\mathbf{r}, t) = -q_0(\mathbf{r}, t), \quad (3)$$

where $\kappa(\mathbf{r})$ is given by

$$\kappa(\mathbf{r}) = \frac{c}{3[\mu_a(\mathbf{r}) + \mu_s'(\mathbf{r})]}, \quad (4)$$

where $\mu_s' = (1 - \bar{f})\mu_s$ is the reduced scattering coefficient; μ_a and μ_s are the attenuation and scattering coefficients, respectively (dimensions of inverse length); and \bar{f} is an anisotropy factor ($0 \leq \bar{f} \leq 1$). Use of the diffusion approximation is widespread, even though it is the simplest approximation to the more general radiative transfer equation and shows significant differences from higher-order approximations such as the diffusive wave approximation.¹² Experimental and theoretical study has demonstrated the validity of Eq. (3) under conditions that are appropriate for the types of application we are considering, where $\mu_a \ll \mu_s$.¹³

We solve Eq. (3) in a domain Ω , with the output flux on the boundary $\partial\Omega$ given by

$$\begin{aligned} \Gamma(\xi; t) &= -\kappa(\xi) \frac{\partial}{\partial n} \Phi(\mathbf{r}, t)|_{\partial\Omega\xi} \\ &= -\kappa(\xi) \hat{\mathbf{n}}(\xi) \cdot \nabla \Phi(\mathbf{r}, t)|_{\partial\Omega\xi}, \end{aligned} \quad (5)$$

where ξ is a point on $\partial\Omega$ and $\hat{\mathbf{n}}(\xi)$ is the outward normal to $\partial\Omega$ at ξ .

A. Green's Function Methods

Because the source q_0 in Eq. (3) is highly localized in both space and time, it approximates a δ function, and

the solution Φ approximates the Green's function for the system, $g(t)$. For time-varying problems this Green's function has been referred to as the temporal point spread function (TPSF).¹ Many authors use very simple geometries such as infinite space, infinite half-space, or infinite slabs, because the temporal Green's function expressions in closed form are simple to compute.¹⁴ More complex geometries such as circles, spheres, and finite and infinite cylinders have been published in closed form,⁹ but these expressions in the time domain are very computationally intensive to calculate, typically involving infinite summations over roots of special functions for every time sample, which presumably explains why the more complex geometries have not been used in data-fitting algorithms.³

B. Finite-Element Methods

In the FEM we find not $\Phi(\mathbf{r}, t)$ [the solution to Eq. (3)], but $\Phi^h(\mathbf{r}, t) = \sum_j^D \Phi_j(t) S_j(\mathbf{r}) \in \Xi^h$, where Ξ^h is a finite dimensional subspace spanned by basis functions $S_j(\mathbf{r})$, $j = 1 \dots D$. The problem becomes one of matrix manipulation:

$$[\mathbf{K}(\kappa) + \mathbf{C}(\mu_a c)]\Phi(t) + \mathbf{B} \frac{\partial \Phi(t)}{\partial t} = \mathbf{Q}(t), \quad (6)$$

where

$$\Phi(t) = [\Phi_1(t), \Phi_2(t), \dots, \Phi_D(t)]^T. \quad (7)$$

We choose basis functions that have limited support so that the $D \times D$ matrices \mathbf{K} , \mathbf{C} , and \mathbf{B} are symmetric, banded, and sparse, and we can use Choleski decomposition with forward and backward substitution to solve the resultant matrix equations.

To find the general behavior of $\Phi(t)$ as a function of time it is standard to use a finite-difference method to integrate Eq. (6).¹⁵ If Φ_n is the solution at time step n , then

$$\begin{aligned} & \left[\theta \mathbf{K}(\kappa) + \theta \mathbf{C}(\mu_a c) + \frac{1}{\Delta t} \mathbf{B} \right] \Phi_{n+1} \\ & + \left[(1 - \theta) \mathbf{K}(\kappa) + (1 - \theta) \mathbf{C}(\mu_a c) - \frac{1}{\Delta t} \mathbf{B} \right] \Phi_n \\ & = \theta \mathbf{Q}_{n+1} + (1 - \theta) \mathbf{Q}_n, \end{aligned} \quad (8)$$

where θ is a parameter used to control the finite-difference method that averages the values at Φ_n and Φ_{n+1} to an intermediate position; we have used the Crank-Nicholson scheme of $\theta = 1/2$.¹⁰ The matrices are constant throughout the finite-difference procedure. Thus the method requires one Choleski decomposition for $(\frac{1}{2}\mathbf{K} + \frac{1}{2}\mathbf{C} + 1/\Delta t \mathbf{B})$, followed by one matrix multiplication and one Choleski forward and backward substitution per time step. Unfortunately, for stability, the time step in the finite-difference procedure needs to be very small $O(10^{-3})$

with respect to the total required TPSF times, and this still leads to quite lengthy computation times.

3. Derivation of the Mellin Transform

A. Green's Function Method

Consider the Mellin transform of the Green's Function:

$$m_n = g^{*(n+1)} = M[g(t); n+1] = \int_0^\infty t^n g(t) dt. \quad (9)$$

For any function

$$\int_{-\infty}^\infty g(t) dt = \sqrt{2\pi} \hat{G}(\omega)|_{\omega=0}, \quad (10)$$

$$\begin{aligned} \frac{\partial^n}{\partial \omega^n} \hat{G}(\omega) &= \frac{1}{\sqrt{2\pi}} \frac{\partial^n}{\partial \omega^n} \int_{-\infty}^\infty g(t) \exp(-i\omega t) dt \\ &= \frac{(-i)^n}{\sqrt{2\pi}} \int_{-\infty}^\infty t^n g(t) \exp(-i\omega t) dt. \end{aligned} \quad (11)$$

If we use the fact that $g(t) = 0$ for $t < 0$, then

$$m_n = i^n \sqrt{2\pi} \frac{\partial^n}{\partial \omega^n} \hat{G}(\omega)|_{\omega=0}, \quad (12)$$

$$\langle t^n \rangle = \frac{m_n}{m_0}. \quad (13)$$

Thus if the analytical form of the Green's function in the Fourier domain is known, the moments are obtained by differentiating with respect to ω and evaluating at $\omega = 0$.

B. Finite-Element Method

1. Zeroth Moment (Time-Independent Case)

We may derive the integrated intensity E directly with

$$[\nabla \cdot \kappa \nabla - \mu_a c] \Phi(\mathbf{r}) = -q_0(\mathbf{r}). \quad (14)$$

Following the above derivation we obtain

$$[\mathbf{K}(\kappa) + \mathbf{C}(\mu_a c)] \Phi = \mathbf{Q}, \quad (15)$$

where \mathbf{K} and \mathbf{C} have the same meaning as before and Φ and \mathbf{Q} now no longer have a time variation.

2. Higher-Order Moments (Time-Dependent Case)

To avoid the finite-difference step, which is the bottleneck in FEM calculations, we make use of the results in Eqs. (10)–(13) to compute the moments directly. Taking the Fourier transform of Eq. (6) yields

$$[\mathbf{K}(\kappa) + \mathbf{C}(\mu_a c) + i\omega \mathbf{B}] \hat{\Phi}(\omega) = \hat{\mathbf{Q}}(\omega). \quad (16)$$

Differentiating with respect to ω yields

$$[\mathbf{K}(\kappa) + \mathbf{C}(\mu_a c) + i\omega\mathbf{B}] \frac{\partial^n \hat{\Phi}(\omega)}{\partial \omega^n} + in\mathbf{B} \frac{\partial^{n-1} \hat{\Phi}(\omega)}{\partial \omega^{n-1}} = \frac{\partial^n \hat{\mathbf{Q}}(\omega)}{\partial \omega^n}. \quad (17)$$

Now if \mathbf{Q} is a δ function in time, then its Fourier transform is a constant, and the right-hand side of Eq. (17) is zero. Evaluating now at $\omega = 0$, we find that

$$[\mathbf{K}(\kappa) + \mathbf{C}(\mu_a c)] \frac{\partial^n \hat{\Phi}(\omega)}{\partial \omega^n} \Big|_{\omega=0} = -in\mathbf{B} \frac{\partial^{n-1} \hat{\Phi}(\omega)}{\partial \omega^{n-1}} \Big|_{\omega=0}, \quad (18)$$

and therefore

$$m_n = n[\mathbf{K}(\kappa) + \mathbf{C}(\mu_a c)]^{-1} \mathbf{B} m_{n-1}. \quad (19)$$

Thus an iterative procedure for finding the set $\{\langle t \rangle, \langle t^2 \rangle, \dots, \langle t^n \rangle\}$ is

1. Solve Eq. (15) for m_0 .
2. Set $n = 1$.
3. Solve Eq. (19) for m_n .
4. $\langle t^n \rangle = m_n / m_0$.
5. $n = n + 1$.
6. Repeat from 3.

4. Results and Discussion

The finite-element model used to obtain the results in this paper comprises a two-dimensional circular mesh formed by triangular elements. The boundary $\partial\Omega$ is assumed to be a polygon. The model is coded in C++ and runs on a Sun Sparc 2 with 32-Mbyte memory. The source is assumed to be isotropic and located at a depth of $1/\mu_s'$ below the surface, at angular position 0° . The Green's function in the Fourier domain for this geometry is given by

$$\hat{G}(\mathbf{r}, \xi, \omega) = \frac{1}{(2\pi)^{3/2} a} \sum_{n=-\infty}^{\infty} \cos(n\theta) \frac{I_n(\alpha r)}{I_n(\alpha a)}, \quad (20)$$

where I_n is the modified Bessel function of the first kind of order n , $\alpha = [(\mu_a c + i\omega)/\kappa]^{1/2}$, a is the radius of the circle, and θ is the angle between the source vector \mathbf{r} and the measurement point ξ on the boundary. The moments can then be derived by application of Eq. (12).

Figure 2 shows a comparison of $\langle t^n \rangle$ for $n = 1, 4$ for analytical results, the results computed from the FEM by the use of the direct method, and the results of deriving the TPSF up to 4 ns and performing the moment integration numerically. The analytic results were calculated with MATHEMATICA.⁹ The two FEM curves are not distinguishable, and instead their relative difference is shown in Fig. 3. Apart

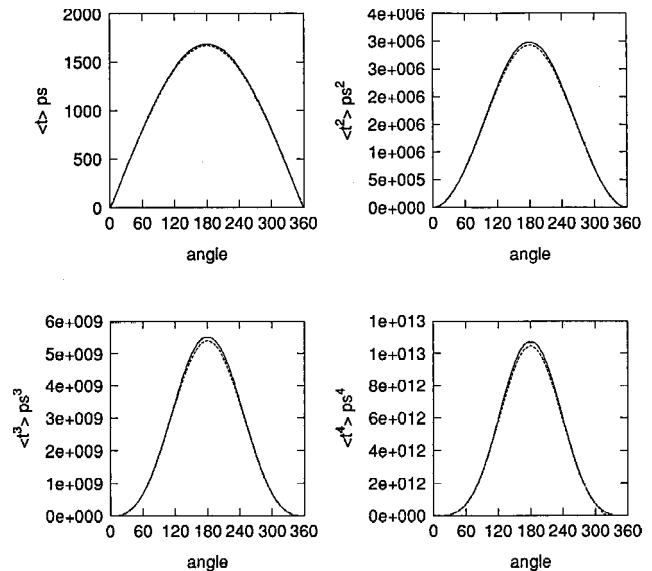


Fig. 2. First four weighted integrals of the TPSF, plotted as a function of angle, for a two-dimensional circle, radius 25 mm, $\mu_a = 0.025 \text{ mm}^{-1}$, $\mu_s' = 2 \text{ mm}^{-1}$. Solid curve, FEM; dashed curve, analytic method.

from positions very close to the source, the results agree to within 0.1%. The difference from the analytical result is only noticeable at large source-detector separations. As expected, skew and kurtosis are both always positive, decreasing with longer distances.

Comparison of timings is shown in Table 1. Note that each time step requires one matrix multiplication followed by one Choleski forward and backward substitution and takes approximately 4.5 s. This should be approximately the same as moment genera-

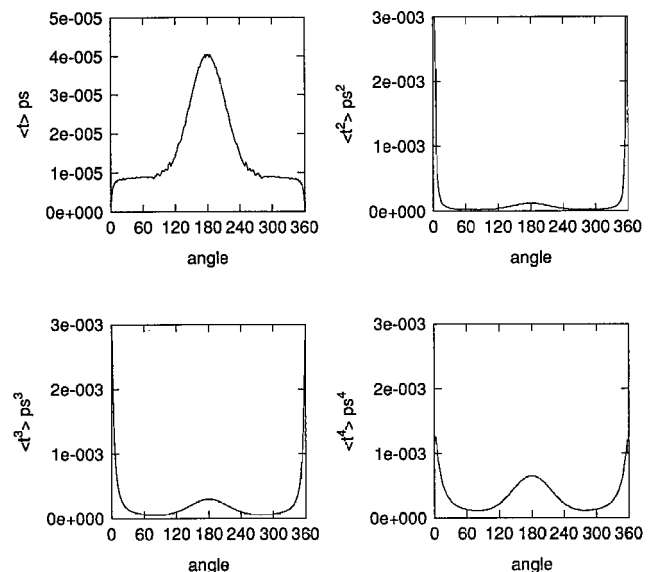


Fig. 3. Relative difference of (direct minus numerically integrated) results for first four weighted integrals of the TPSF for the same parameters as in Fig. 2.

Table 1. Time in Seconds for FEM Calculations^a

FEM Setup Time (s) ^b	Time- Resolved ^c	Moment									
		0	1	2	3	4	5	6	7	8	
134	5290	4.5	14	23	33	42	51	61	70	80	

^a25-mm-radius two-dimensional mesh with 3350 nodes and 6512 elements; $\mu_a = 0.025 \text{ mm}^{-1}$, $\mu_s' = 2 \text{ mm}^{-1}$.

^bSetup time was for geometry and matrix assembly calculations.

^cTime-resolved figure was for 800 time steps.

tion, but in fact the latter is approximately twice as long because of some inefficiencies in the current implementation.

It is worth pointing out that the setup time is a constant for the mesh and is only done once. After this all repetitions of the moment calculations, including those for different source positions, take only the time indicated under the moment index in Table 1. On progressing to three-dimensional meshes, we typically find the need for 60000 to 70000 elements—an increase of tenfold. The commensurate increase in matrix manipulation time may be 100 times, leading to several minutes per calculation; for generation of $\Gamma(t)$ we would expect several days of computation, a time comparable with Monte Carlo methods. Whereas a time of a few minutes is not intolerable, some optimization may be necessary to bring the speed of calculation to a more acceptable level. We are currently investigating a number of these optimization schemes. In any case the cost of moment generation will remain an order of magnitude less than that for the full TPSF.

5. Conclusions

For analysis of photon time of flight in tissue it is essential to have efficient computational methods. We have presented a computational method that exploits the operator representation of FEM matrices to yield the Mellin transform of the TPSF directly, and thence its moments. The moments are important not only to provide a representation of the TPSF itself, but to provide a robust statistic. The moments show far greater stability over integrated intensity or early light, as well as greater sensitivity of signal to noise in perturbation studies that are the basis for image reconstruction. The computational speed up is several orders of magnitude, making near-real-time computation of simulated photon transport possible in two dimensions. For three dimensions the improvement is expected to be even more essential. In addition it is hoped that further theoretical developments may yield yet faster methods.

This work was supported by the Engineering and Physics Research Council, The Wellcome Trust, and Hamamtsu Photonics KK.

References

1. D. T. Delpy, M. Cope, P. van der Zee, S. R. Arridge, S. Wray, and J. Wyatt, "Estimation of optical pathlength through tissue from direct time of flight measurement," *Phys. Med. Biol.* **33**, 1433–1442 (1988).
2. B. Chance, J. S. Leigh, H. Miyake, D. S. Smith, S. Nioka, R. Greenfield, M. Finander, K. Kaufman, W. Levy, M. Young, P. Cohn, H. Yoshioka, and R. Boretsky, "Comparison of time-resolved and unresolved measurements of deoxyhemoglobin in brain," *Proc. Nat. Acad. Sci. USA* **85**, 4971–4975 (1985).
3. S. J. Madsen, M. S. Patterson, B. C. Wilson, Y. D. Park, J. D. Moulton, S. L. Jaques, and Y. Hefetz, "Time-resolved diffuse reflectance and transmittance studies in tissue simulating phantoms: a comparison between theory and experiment," in *Time-Resolved Spectroscopy and Imaging of Tissues*, B. Chance and A. Katzir, eds., *Proc. Soc. Photo-Opt. Instrum. Eng.* **1431**, 42–51 (1991).
4. S. R. Arridge, P. van der Zee, M. Cope, and D. T. Delpy, "Reconstruction methods for infrared absorption imaging," in *Time-Resolved Spectroscopy and Imaging of Tissues*, B. Chance and A. Katzir, eds., *Proc. Soc. Photo-Opt. Instrum. Eng.* **1431**, 204–215 (1991).
5. B. C. Wilson and G. Adam, "A Monte-Carlo model for the absorption and flux distribution of light in tissue," *Med. Phys.* **10**, 824–830 (1983).
6. P. van der Zee and D. T. Delpy, "Simulation of the point-spread function for light in tissue," *Adv. Exp. Med. Biol.* **215**, 179–192 (1987).
7. S. T. Flock, M. S. Patterson, B. C. Wilson, and D. R. Wyman, "Monte Carlo modelling of light propagation in highly scattering tissues—I: Model predictions and comparison with diffusion theory," *IEEE Trans. Biomed. Eng.* **36**, 1162–1168 (1989).
8. R. F. Bonner, R. Nossal, R. Havlin, and G. H. Weiss, "Model for photon migration in turbid biological media," *J. Opt. Soc. Am. A* **4**, 423–432 (1987).
9. S. R. Arridge, M. Cope, and D. T. Delpy, "The theoretical basis for the determination of optical pathlength in tissue: temporal and frequency analysis," *Phys. Med. Biol.* **37**, 1531–1560 (1992).
10. S. R. Arridge, M. Schweiger, M. Hiraoka, and D. T. Delpy, "A finite element approach for modeling photon transport in tissue," *Med. Phys.* **20**, 299–309 (1993).
11. S. R. Arridge and M. Schweiger, "The use of multiple data types in Time-resolved Optical Absorption and Scattering Tomography (TOAST)," in *Mathematical Methods in Medical Imaging II*, D. C. Wilson and J. N. Wilson, eds., *Proc. Soc. Photo-Opt. Instrum. Eng.* **2035**, 218–229 (1993).
12. J. P. Kaltenbach and M. Kaschke, "Frequency- and time-domain modeling of light transport in random media," in *Medical Optical Tomography: Functional Imaging and Monitoring*, G. Muller, G. Müller, B. Chance, R. Alfano, S. Arridge, J. Beuthan, E. Gratton, M. Karchke, B. Masters, S. Svonberg, and P. Van der Zee, eds. (Society of Photo-Optical and Instrumentation Engineers, Bellingham, Wash., 1993), pp. 65–86.
13. R. A. J. Groenhuis, H. A. Ferwada, and J. J. Ten Bosch, "Scattering and absorption of turbid materials determined from reflection measurements (parts 1 and 2)," *Appl. Opt.* **22**, 2456–2467 (1983).
14. M. S. Patterson, B. Chance, and B. C. Wilson, "Time resolved reflectance and transmittance for the non-invasive measurement of tissue optical properties," *Appl. Opt.* **28**, 2331–2336 (1989).
15. G. Strang and G. J. Fix, *An Analysis of the Finite Element Method* (Prentice-Hall, Englewood Cliffs, N.J., 1973).